

SHP-1 regulates T cell adhesion by activating CrkII in the immunological synapse

Inbar Azoulay-Alfaguter¹, Marianne Strazza¹, Michael Peled¹, Hila K. Novak^{2,3}, James Muller²,
Michael L. Dustin^{2,3}, Adam Mor^{1,2,4,*}

T cell receptor controls Rap1 activation and T cell adhesion by recruiting SHP-1 to the immunological synapse.

¹ Department of Medicine, New York University School of Medicine, New York, NY, USA

² Department of Pathology, New York University School of Medicine, New York, NY, USA

³ Kennedy Institute for Rheumatology, Oxford University, Oxford, UK

⁴ Perlmutter Cancer Center, New York University School of Medicine, New York, NY, USA

* Corresponding to Dr. Adam Mor, 450 East 29th Street, Room 806, New York, NY 10016. Tel.: 646-501-4516. E-mail: Adam.Mor@NYUMC.org

Abstract

The adaptor protein CrkII is a key regulator of T cell adhesion through the recruitment of the Rap1-guanine exchange factor, C3G. Subsequently, Rap1 activates the integrin LFA-1 leading to T cell adhesion and interaction with antigen presenting cells (APC). The interphase between T cell and APC is known as the immunological synapse (IS). It is characterized by specific organization of proteins that can be divided into central supramolecular activation clusters (c-SMAC) and peripheral supramolecular activation clusters (p-SMAC). Using TIRF microscopy and support lipid bilayers we determined that activated Rap1 was recruited to the IS. Within the IS, Rap1 was localized to the p-SMAC. C3G and the active (dephosphorylated) form of CrkII were also localized to the same compartment. In contrast, inactive (phosphorylated) CrkII was limited to the c-SMAC. We then showed that activation of CrkII and subsequent trafficking from the c-SMAC to the p-SMAC were regulated by the phosphatase SHP-1 downstream of the antigen receptor. In the p-SMAC, CrkII recruited C3G, leading to Rap1 activation and LFA-1 mediated adhesion. Functionally, SHP-1 was necessary for both adhesion and migration of T cells. Thus, we uncovered a new signaling pathway where SHP-1 acts through CrkII to reshape the pattern of Rap1 activation in the IS.

Introduction

T lymphocytes are central to the responses of the adaptive immune system, both beneficial and malign (1, 2). Adhesion is an essential aspect of T cell biology; without proper adhesion, T cells can neither traffic to appropriate compartments, nor recognize antigens presented on major histocompatibility complexes (3). Effective T cell adhesion is also essential for autoimmunity, suggesting that adhesive function may be a target for treating diseases such as rheumatoid arthritis, lupus, and psoriasis (3). However, the potential for therapeutically ameliorating autoimmune conditions by modulating T cell adhesion has thus far been limited by adverse events (3). To identify more selective control points, it is imperative to better understand the molecular mechanisms regulating T cell adhesion (4-6).

LFA-1 is a critical adhesion molecule for T cell interactions with antigen presenting cells (APC) (7). LFA-1 affinity for its counter-ligand, intercellular adhesion molecule-1 (ICAM-1), varies with activation state, and is determined by the small GTPase Rap1 (8) and the organization of the actin cytoskeleton (9). The ability of Rap1 to control LFA-1 affinity for ICAM-1, and thus T cell adhesion, is established, though the pathway between the TCR and Rap1 is incompletely elucidated (Fig. 1) (10). The physiological relevance of Rap1 is evident in patients suffering from a congenital defect in Kindlin-3, required for proper Rap1 signaling (11, 12). Such patients manifest leukocyte-adhesion deficiency type III syndrome, an immunodeficiency and blood clotting disorder (13). Rap1 cycles between active (GTP-bound) and inactive (GDP-bound) conformations (8, 14). As for all small GTPases, Rap1 activation is regulated by guanine nucleotide exchange factors (GEF) that induce Rap1 to release GDP in favor of GTP-binding and by GTPase-activating proteins (GAP) that enhance the slow intrinsic GTPase reaction (8, 15).

One important Rap1 GEF is C3G, which is highly expressed in T lymphocytes (16, 17). The C-

terminus of C3G consists of the CDC25 homology domain, which is the catalytic domain of the Ras-family. The N-terminal region of C3G negatively regulates its GEF activity. Following translocation from the cytosol to the cell membrane (18), C3G becomes phosphorylated on tyrosine 504 (16), and the negative regulation by its N-terminal region is repressed to increase the GEF activity.

The adaptor protein CrkII is essential for C3G function (16). It is involved in the early steps of lymphocyte activation through its SH2-mediated interaction with proximal signal proteins such as Cbl, Zap70, CasL, and STAT5 (19). In addition, it constitutively associates, via its SH3 domain, with C3G. Recent studies demonstrated that the conformation and function of CrkII is subjected to regulation by immunophilins (20), which also affects CrkII-dependent T cell adhesion and migration (21). Using conditional knockout mice, the Burkhardt lab has reported that T cells lacking CrkII exhibit reduced integrin mediated adhesion and chemotaxis (22). They also determined that CrkII coordinated C3G to activate Rap1 (22). While this work does convincingly establish a role for CrkII in selective regulation of T cell adhesion and migration at effector sites, the implication of C3G as the GEF downstream the TCR is indirect in linking a decrease in C3G phosphorylation downstream of chemokine signaling to the observed decrease in Rap1 activation in CrkII deficient cells.

The immunological synapse (IS) describes stable, antigen specific adhesive junctions formed between T cells and APCs, which may include well organized supramolecular activation clusters (SMAC) (23). SMACs comprise concentric rings that each contains segregated clusters of proteins driven by TCR signaling. The central-SMAC (c-SMAC) is enriched in co-stimulatory receptors such as CD28, the peripheral-SMAC (p-SMAC) is enriched in LFA-1-ICAM-1 interactions, and the distal-SMAC (d-SMAC) is enriched in F-actin and the transmembrane phosphatase CD45 (24). These structures are found at the interface between two cells (such as

APC and T cell), but can be modeled using a supported lipid bilayer (SLB) with proteins that diffuse within the bilayer in place of the APC. Total internal reflection fluorescence (TIRF) microscopy is ideal for high contrast imaging of fluorescently tagged molecules involved in IS formation in the SLB system. In single activated T cells, our group and others have reported that the activated pool of Rap1 decorates both the plasma membrane and the vesicular compartments (18, 25, 26). However, the distribution of Rap1 within different compartments of the IS, its interaction with proximal signaling components in this setting, as well as its functions and contribution to productive synapses is unknown.

The main aim of this work was to uncover the biology of Rap1 in the IS. Using TIRF microscopy we discovered that both Rap1 and the exchange factor C3G were localized to the p-SMAC. Moreover, we showed that dephosphorylation of the adaptor protein CrkII downstream of the TCR regulated C3G activity and subsequent Rap1 activation. Importantly, dephosphorylation of CrkII was mediated by the phosphatase SHP-1 and contributed to multiple T cell functions including adhesion, migration, and cytokine secretion.

Results

Activated Rap1 is recruited to the immunological synapse

We, in addition to others (8), have shown that ligation of the TCR with anti-CD3 antibody resulted in activation of Rap1 at the plasma membrane (14, 25-27). One of the main characteristics of IS formation is polarization and recruitment of proximal signaling proteins towards the contact area. A recent study from the Altman lab documented recruitment of Rap1 to the IS in fixed cells, but whether this pool of Rap1 is activated (GTP bound) is not clear (26). To find out where in the cell Rap1 is activated during IS formation we utilized Jurkat T cells expressing GFP-RalGDS-RBD (a probe for activated Rap1) co-cultured with Raji B cells preloaded with staphylococcus enterotoxin E (SEE). As shown, Rap1 activation in live cells was

limited to the contact area between the cells in 82% of the stable conjugates (Fig. 2A lower panel). Polarized Rap1 recruitment was specific to signals delivered via the TCR since Rap1 was recruited to the contact area in the absence of SEE in only 16% of cells forming stable conjugates (Fig. 2A upper panel and Fig. S1).

Because antibody mediated stimulation diminishes the potential physiological relevance, we confirmed the recruitment of GTP loaded Rap1 to the IS also by activating T cells with natural ligands expressed by APCs. Specifically, we co-cultured OT-II T cells (26) expressing GFP-RalGDS-RBD with dendritic cells (DC) loaded with OVA peptide. As shown, activated Rap1 was enriched in the contact area of 65% of the cells stimulated via the TCR (Fig. 2B), suggesting that Rap1 activation occurs at the IS of primary murine T cells as well.

In order to resolve the distribution of Rap1 in the IS we utilized the SLB model and TIRF microscopy (Fig. 2F). When primary human T cells were added to bilayer containing anti-CD3 antibody and recombinant ICAM-1, Rap1 was excluded from the c-SMAC in both early (5 minutes) and late (20 minutes) synapses (Fig. 2C and 2D). To show that this exclusion was not secondary to physical retraction, we tether GFP to the plasma membrane (GFP-CAAX) and showed expression in both compartments (Fig. S2). Interestingly, the closely related GTPase Ras (17) was not excluded from the c-SMAC (Fig. 2C and 2D). Perhaps more striking was the fact that while the pool of activated (GTP loaded) Rap1 was also excluded from the c-SMAC, GTP loaded Ras demonstrated strong accumulation in the c-SMAC (Fig. 2C and 2E). Thus, activated Rap1 is polarized to the contact area during synapse formation.

What are the factors regulating Rap1 localization in the immunological synapse?

The ability of Rap1 to interact with lipid membranes is by virtue of the attachment of geranylgeranyl lipid to its hyper-variable region as well as by the affinity of its adjacent positively charged sequence to the inner leaflet of the plasma membrane (28-30). When we cloned and expressed a version of Rap1 in which the 20-carbon geranylgeranyl lipid tail was replaced by the 15-carbon prenyl group of Ras (by changing the CAAX domain in the hyper-variable region into CVVM) (Fig. S3), Rap1 lost its unique distribution, and was not excluded from the c-SMAC (Fig. 3A and 3B), suggesting that 20- (and not 15-), carbon tail of Rap1 is required for its compartmentalization within the IS.

Previously we showed that Rap1 was localized to the plasma membrane and by using the RalGDS-RBD probe we also demonstrated that this pool of Rap1 was GTP loaded (Fig. 2). To identify whether the activation status of Rap1 (GTP vs. GDP) contributes to its localization in the IS, we overexpressed activated (Rap1V12) and inactivated (Rap1N17) versions of Rap1 in primary human T cells to find that despite similar expression levels (Fig. S4) the activated pool of Rap1 was excluded from the c-SMAC, while the inactivated pool of Rap1 failed to decorate the IS at all (Fig. 3A and 3C). This is an important finding, suggesting that despite the fact that there is a plasma membrane pool of inactivated Rap1 (GFP-Rap1 and GFP-RalGDS-RBD do not share the same subcellular distribution in activated cells), the pool in the IS is exclusively GTP loaded.

It is appreciated that the subcellular localization of multiple small GTPases is determined by the distribution of their specific GEFs and GAPs (15, 31). As shown, the major GEF for Rap1 in T cells, C3G (either wild type (C3G) or activated C3G (C3G Y504D)), was also excluded from the c-SMAC (Fig. 3A and 3D). This is unique to C3G because another Rap1 GEF, CalDAG-GEFIII (15, 32), failed to show the similar distribution (Fig. 3A and 3D). While it is not surprising that

C3G is localized to the IS, why it is excluded from the c-SMAC (unlike other GEFs) is unclear. Thus, multiple process such as lipidation, activation, and the presence of specific GEF contribute together to proper Rap1 localization in the IS.

CrkII localization in the immunological synapse is regulated by phosphorylation

CrkII is an adaptor protein that binds to several tyrosine phosphorylated proteins and is required for proper localization of the GEF C3G (20, 21, 33, 34). While we validated the ability of dephosphorylated CrkII to interact with C3G (Fig. S5A and S5B), the Isakov group has found that the binding between these proteins, and subsequent T cell adhesion, was regulated by the peptidyl-prolyl isomerases immunophilins (20). Upon phosphorylation, CrkII folds on itself to cover its SH2/SH3 binding sites and thus become inactive (21, 35) (Fig. 4A). While the phosphodeficient (active) version of CrkII (CrkII Y221A) was recorded at the same location as C3G (Fig. 4B and 3A) and Rap1 (Fig. 2C), the phosphomimetic (inactive) version of the same protein (CrkII Y221D) was restricted to the c-SMAC in primary human T cells (Fig. 4B and 4C). To further support this finding, and to validate that wild type CrkII could translocate between different compartments of the IS dependent on its phosphorylation status, we treated cells expressing CrkII with pervanadate, a tyrosine phosphatase inhibitor (36), and documented its distribution (Fig. 4D). Despite the fact that this treatment leads to phosphorylation of multiple proteins, using a specific antibody we confirmed that CrkII was among them and that it occurred at position 221 (Fig. S6A and S6B). We found that within 10 minutes of treatment, CrkII redeployed from the p-SMAC to the c-SMAC in the majority of the cells, presumably after phosphorylation at position 221 (Fig. 4D and 4E). Altogether, our data demonstrate that dephosphorylated CrkII travels to the periphery of the IS, where it can probably act on its effector C3G.

CrkII dephosphorylation regulates T cell activation

An important aim in our search to identify CrkII upstream signaling elements was to uncover the mechanism by which CrkII is dephosphorylated prior to its relocation to the p-SMAC. Since CrkII is also a cytosolic protein, we first demonstrated that there was an increase in the levels of this protein in the membrane fraction upon TCR ligation (Fig. S7A and S7B). The same treatment also resulted in reduction of the levels of phosphorylated CrkII at two different time points (Fig. 5A and 5B). To validate this finding using additional imaging approach we expressed the PICCHUx vector (YFP-CrkII-CFP-CAAX) in T cells treated with anti-CD3 antibody (20). This FRET based vector was designed to report the folding status of CrkII (37). There was a reduction in FRET efficiency upon stimulation of transiently transfected Jurkat cells (Fig. 5C and 5D), suggesting that engagement of the TCR resulted in dephosphorylation of CrkII. To show that CrkII dephosphorylation is associated with increase adhesion we expressed phosphodeficient and phosphomimetic versions of CrkII in T cells and demonstrated that only the former resulted in a higher level of GTP-Rap1 and in increased adhesion to ICAM-1 coated surfaces (Fig. 5E and 5F). To confirm that CrkII Y221D was folded properly we cloned and expressed phosphomimetic and phosphodeficient versions of the PICCHUx vector (YFP-CrkII Y221D-CFP-CAAX and YFP-CrkII Y221A-CFP-CAAX respectively) and confirmed high FRET efficiency in the latter (Fig. S8A and S8B). To demonstrate the contribution of phosphodeficient (active) CrkII to cellular functions, we expressed CrkII Y221A in T cells stimulated with anti-CD3 antibody in wells coated with ICAM-1 (to mimic the IS environment) (38) and identified an increase in the expression levels of the activation marker CD69 (Fig. 5G purple histogram). CrkII Y221A also enhanced interleukin (IL)-2 release in response to the same treatment (Fig. 5H) (8, 39, 40). These findings suggest that ligation of the TCR leads to dephosphorylation of CrkII that is associated with increased adhesion to ICAM-1, cellular activation, and IL-2 secretion.

SHP-1 dephosphorylates CrkII downstream of the T cell receptor

To uncover the signaling events between the TCR and CrkII dephosphorylation we treated Jurkat T cells with two phosphatases inhibitors (NSC-87877; non-specific SHP1/2 inhibitor (41) and cantharidic acid; PP2 inhibitor (5, 42)), and measured the levels of phosphorylated CrkII upon treatment with anti-CD3 antibody. Remarkably, only treatment with NSC-87877 resulted in higher levels of phosphorylated CrkII (Fig. 6A). The same treatment also resulted in inhibited adhesion of anti-CD3 antibody treated cells to ICAM-1 coated wells (Fig. 6B). This pattern of inhibition was rescued by overexpressing phosphodeficient CrkII (CrkII Y221A), suggesting that at least one of the targets for SHP1/2 is the adaptor protein CrkII (Fig. 6B). There are two main isoforms of SHP: SHP-1 and SHP-2 (43). Both are member of the protein tyrosine phosphatase family. SHP-1 and SHP-2 are widely expressed in most tissues and play a regulatory role in various cell signaling events that are important for a diversity of cell functions, such as mitogenic activation, metabolic control, and cell migration (44). When we knocked down each isoform individually (Fig. 6C) and measured the levels of phosphorylated CrkII, SHP-1 (and not SHP-2) played a more significant role downstream of the TCR (Fig. 6D and 6E). Moreover, knocking down SHP-1 inhibited TCR induced static adhesion (45) to ICAM-1 in both Jurkat T cells expressing the relevant shRNA (Fig. 6F), and in primary human T cells treated with siRNA (Fig. 6G). To confirm that the contribution of SHP-1 to adhesion was not secondary to SHP-2 signaling, both enzymes were knocked down simultaneously and adhesion to ICAM-1 was performed. As shown, knocking down SHP-1 alone, or SHP-1 together with SHP-2 inhibited adhesion to the same extent (Fig. 6G). To rule out off-target effects related to our inhibitory RNAs, we rescued the adhesion defect of the cells by overexpressing GFP tagged SHP-1 (Fig. 6H). The contribution of SHP-1 to TCR signaling was also demonstrated by a chemokinesis assay (46), where primary human T cells deficient in SHP-1 failed to arrest after crosslinking of the antigen receptor (Fig. 6I). Using conjugate formation assay we demonstrated that SHP-1 was required for activation and recruitment of Rap1 to the contact area of Jurkat T cells (Fig. 5J) and of primary human T cells cocultured with APCs (Fig. 5L). Moreover, SHP-1 was also required

for the increase in the percentage of stable conjugates (Fig. 5K). Altogether, our results suggest that CrkII is targeted by SHP-1 upon TCR stimulation, and that SHP-1 is required for Rap1 activation and T cell adhesion downstream to the antigen receptor.

Discussion

Previous work has shown that Rap1 activation upon TCR signaling is regulated primarily by the exchange factor C3G (40, 47). C3G was the first Rap1 GEF identified and is highly expressed in T lymphocytes. It transduces signals from Crk proteins, binding to their SH3 domain and activating mainly Rap1 (and to a lesser extent also other members of the Ras family of GTPases). C3G recruitment to the plasma membrane is facilitated by several adaptor proteins, including CrkII, CrkL, and CasL (48, 49). Unlike C3G that is restricted to the p-SMAC, CrkII travels from the p-SMAC to the c-SMAC upon its phosphorylation (Fig. 7).

Compartmentalization of signaling molecules to different areas of the IS based on their phosphorylation has been reported. Campi et al reported that phosphorylated TCR clusters move to the c-SMAC (50) and Davis et al discovered that phosphorylated LAT clusters and vesicles move centripetally during synapse formation (51, 52). Analogously, we show here that the phosphorylation status of CrkII is directly linked to its compartmentalization within the IS. Interestingly, the direction of its trafficking is not to, but rather away from the center of the synapse. Moreover, the localization of CrkII is also associated with multiple T cell functions including adhesion and cytokine secretion. This is an example of how subcellular localization of an adaptor protein can regulate downstream signaling (51, 53).

An additional level of CrkII regulation was demonstrated by previous studies showing an important role for the proline rich domain, and its ability to alter CrkII from a cis (inactive) to a trans (active) conformation (54, 55). In this regard, the Isakov group has shown that the binding

of CrkII to C3G was enhanced by prolyl-isomerase activity (20, 56, 57). The contribution of CrkII isomerization to its localization at different compartments of the IS is not clear.

An important issue is the mechanism that retains dephosphorylated CrkII at the p-SMAC. It has been reported previously that the adaptor protein CasL was limited to that compartment (49, 58) and we have validated that CrkII and CasL physically interact (Fig. S5C and S5D), suggesting that CasL might be a docking site to retain CrkII in the periphery of the synapse where it can signal downstream to Rap1 and to LFA-1 (Fig. 7). Interestingly, and in contrast to CrkII, the TCR complex travels to the center of the synapse upon stimulation and during the maturation process. While CrkII trafficking is regulated by dephosphorylation and possibly binding to CasL, the contribution of Rap1 and Ras signaling to TCR trafficking remains incompletely understood. Choudhuri et al has recently reported that polarized vesicles enriched with TCR complexes emerge from the center of the synapses (59). Whether these vesicles are also enriched with activated Rap1 or Ras proteins is under active investigation in our laboratory.

Tyrosine phosphorylation (and dephosphorylation) of proteins plays a critical role in many T cell functions (43). The opposing actions of kinases and phosphatases determine the level of tyrosine phosphorylation at any given time (60, 61). It is well appreciated that kinases are essential during T cell signaling to adhesion. Billadeau et al very clearly demonstrated that although the kinase Abl did not regulate the recruitment of C3G to the IS, it affected the phosphorylation of C3G itself, which was required for its GEF activity toward Rap1 (40). The role and significance of phosphatases to T cell functions are less appreciated (43). Specifically, the role of the phosphatases SHP-1 and SHP-2 in T cells is not clear due to numerous opposing reports showing that SHP-2 activity is related to activating pathways (62), while SHP-1 is associated with inhibition of selected T cell functions (43). Analogues to the mechanism by which the

phosphatase CD45 activates Lck, our data demonstrate that SHP-1 targets CrkII upon TCR stimulation, leading to C3G recruitment and Rap1 induced LFA-1 activation in the IS (Fig. 7). Thus, our study reveals a novel function for SHP-1 in integrin-mediated adhesion downstream of the TCR.

Despite a high degree of homology between Ras and Rap1, their localization in the IS was very different. Whereas activated Ras was limited to the c-SMAC, GTP-loaded Rap1 was excluded from the same compartment. We hypothesize that this is secondary to the differences in the sequences of the hyper-variable regions of these GTPases, leading to diverse post-translational modifications that ultimately support affinity to either the p-SMAC or the c-SMAC. Ongoing experiments in our lab will clarify these findings.

Another observation that was not addressed in this work is the unique pattern of distribution of CrkII and C3G. Both demonstrated tight cluster organization (Fig. 3A and Fig. 4B) within the IS. These clusters resemble talin micro clusters (63), suggesting a possible interaction with the actin cytoskeleton (9, 64) or with other actin regulatory proteins such as WASP (65, 66), SKAP (67, 68), RapL (14), RIAM (15, 69), or WAVE2 (40). The role of the actin cytoskeleton and / or these proteins in CrkII dynamics will be a subject for future studies. Specifically, it has been reported recently that the protein SLAT was crucial for TCR-induced LFA-1 activation and T cell adhesion (26). Interestingly, SLAT interacts, through its PH domain, with activated Rap1. This interaction has been shown to facilitate the recruitment of Rap1 and SLAT to the IS (26). The distribution of SLAT within different compartments of the synapse is of interest.

Altogether our data show a novel regulatory pathway leading to T cell adhesion. TCR activation induces dephosphorylation of plasma membrane CrkII by SHP-1. Dephosphorylated CrkII translocates to the p-SMAC. In the p-SMAC, CrkII interacts with C3G that activates Rap1. Thus, we

position CrkII and SHP-1 as critical players in synapse formation to suggest that manipulating CrkII phosphorylation might serve as a target to treat inflammatory diseases.

Material and Methods

General reagents

RPMI 1640 and Opti-MEM-I were purchased from Invitrogen. Poly-l-lysine was purchased from Sigma. Staphylococcus enterotoxin E was purchased from Toxin Technology (Sarasota, FL). BCA assay was purchased from Pierce Biotechnology. Prevanadate was prepared by mixing orthovanadate (Sigma) and H₂O₂ (Sigma) at 1:1 ratio and used at final concentration of 50 μ M. NSC-87877 was purchased from Millipore and Cantharidic acid was obtained from Santa Cruz.

Cell culture, transfection, and stimulation

Jurkat T cells and Raji B cells were obtained from the American Type Culture Collection. Cells were maintained in 5% CO₂ at 37°C in RPMI 1640 media supplemented with 10% FBS and 1% Pen/Strep. 293T cells were obtained from the American Type Culture Collection and maintained in 5% CO₂ at 37°C in DMEM media supplemented with 10% FBS and 1% Pen/Strep. Human peripheral untouched CD3 T lymphocytes were isolated from whole blood using Rosettesep™ human CD3 T cell isolation kit (Stemcell Technologies), followed by separation over density gradient medium (Lymphoprep™; Stemcell Technologies). Primary cells were maintained in enriched media containing 1% L-glutamine, 1% non-essential amino acids, 1% sodium pyruvate, and 1% HEPES at 5% CO₂ and at 37°C. Constructs were introduced into Jurkat, primary human, and primary mouse T cells by nucleofection (Lonza), while transfection efficiency of 50-70% was achieved in all experiments. Immobilized or soluble anti-CD3 (1-5 μ g/ml) antibody and ICAM-1 (250 molecules/mm²) were used for stimulation. Constructs were introduced into 293T cells by SuperFect transfection reagent (Qiagen) according to the manufacturer's protocol.

Antibodies and recombinant proteins

Anti-CD3 (BioLegend), anti-CD3, anti-CD28 (Ancell), anti-pCrkII (Tyr 221; Cell Signaling), anti-CrkII (Santa Cruz), anti-RhoGDI (BD Biosciences), anti-C3G (Bethyl laboratories), anti-SHP-1 (SH-PTP1) / SHP-2 (SH-PTP2) Abs (Santa Cruz), anti-phosphotyrosine (4G10; Millipore), anti-Rap1 (Millipore), anti-GFP mAb-Agarose (MBL), anti-GFP (Invitrogen), anti-HA (Abcam), anti-CD69 PE (eBioscience) antibodies were purchased as described. Monobiotinylated and Alexa 568 (Invitrogen) anti-CD3 ϵ Fab' (UCHT1) and ICAM-1-His12 AF 405 were generated as previously described (59). In solid phase stimulation experiments recombinant human ICAM-1-Fc (R&D) was utilized.

DNA expression constructs

GFP-C3G was a gift from Philip Stork (The Vollum Institute). Cherry-Rap1, GFP-RBD-RalGDS, GFP-Rap1, GFP-N-Ras, GFP-Raf1-RBD, GFP-Rap1V12, GFP-Rap1N17, GFP-C3G-Y504V, and CalDAGGEFIII constructs were previously described (18, 25, 70, 71). GFP-CrkII was provided by Kenneth Yamada (AddGene). GFP-Rap1-CVVL, CrkII Y221A, and CrkII Y221D were cloned by an overlapping PCR (primers sequences are available upon request). PICCHUx vector was a gift from Michiyuki Matsuda (Osaka University). Flag-CasL-HA was provided by Lynda Chin (AddGene). SHP-1-MSCV-IRES-GFP vector was a gift from Ben Neel (NYU). Plasmids were treated with an UltraClean endotoxin removal kit (MO BIO Laboratories) and verified by bidirectional sequencing.

Conjugate formation assay

Staphylococcus Enterotoxin E (SEE) loaded Raji B cells (1.5×10^6) were mixed with Jurkat T cells (1.5×10^6), plated on poly-L-lysine (10 $\mu\text{g/ml}$) coated glass bottom culture 35mm plates (ibidi GmbH), and subjected to brief centrifugation prior to imaging. Images were taken with Zeiss 700

confocal microscope and quantified for conjugate formation as previously described (5, 6) (Fig. S2). OT-II T cells expressing a transgenic TCR that recognizes OVA were isolated from single-cell spleen suspensions of DO11.10 mice by depletion of magnetically labeled non-CD3 cells (Invitrogen). To isolate APCs, spleen suspensions were prepared by digestion with collagenase D (100 U/ml) in HBSS for 40 min. Low-density cells were isolated by centrifugation over a 60% Percoll gradient. Cells were further enriched by differential adherence by incubating cells on 100-mm tissue culture plates in medium containing 5% FBS for 2 hours with 100 µg/ml OVA peptide.

Lipid bilayer experiments

Lipid bilayers were prepared as previously described (72). Liposomes that containing biotin-CAP-phosphatidylethanolamine, phosphatidylcholine, and Ni^{2+} chelating lipids (Avanti Polars Lipids) were placed on Piranha solution (Cyantek corporation) cleaned 40 mm glass coverslip to form the planar bilayers. Following blocking for 30 minutes with 5% casein, 100 µM NiCl_2 , fluorescently labeled His-ICAM-1 (250 molecules/ mm^2), and monobiotinylated Fab' fragments of human CD3 ε antibodies (5 µg/ml), flow chambers were warmed up to 37°C and cells expressing the relevant constructs were injected in 200 µl of HEPES-buffered saline containing 1% human serum albumin (Sigma). Images were collected at different time points. For immunostaining, cells were fixed using 2% paraformaldehyde at room temperature for 20 minutes and permeabilized with 0.1% Triton X-100 for 1 minute. Cells were then blocked using 5% casein for 30 minutes, washed and incubated with primary antibodies for 30 minutes and appropriate secondary antibodies for additional 20 minutes.

Microscopy

TIRF microscopy imaging was performed on the custom automated Nikon inverted fluorescence microscope using the 100×/1.45 N.A objective. TIRF illumination was set up and aligned

according to the manufacturer's instructions as previously described (72). Confocal microscopy was carried out on a Zeiss LSM 700 system (Carl Zeiss).

Chemokinesis assay

CHO-ICAM-1 cells (ATCC) were plated on fibronectin coated glass bottom μ -dishes (ibidi) and grown overnight until confluent. siRNA targeting SHP-1 or SHP-2 (Dharmacon ON-TARGET SMARTpool) were introduced into primary human T cells by nucleofection (Lonza). Cells were labeled with CFSE and plated onto the CHO-ICAM-1 monolayers. Cells were allowed to settle for 3 minutes prior to the addition of anti-CD3 antibody (1 ug/ul). Immediately following stimulation cells were live-imaged, a series of 30 images were captured over 10 minutes with an inverted Zeiss 700 laser scanning confocal microscope (Carl Zeiss Microimaging), and cell movement was analyzed by Volocity Software (Version 6.2.1).

Rap1 activation assay

Activated Rap1 was detected by the GST pull-down assay, as previously described (5). Jurkat T cells were stimulated with anti-CD3 antibody for 2 minutes prior to cell lysis. Cell lysates were incubated with GST-RBD-RalGDS coupled to glutathione beads to pull down activated Rap1. Pull-down lysates were then separated by tris-glycine PAGE and transferred to nitrocellulose filters. Blots were blocked and incubated with the anti-Rap1 antibody at 4°C overnight. Immunoreactive bands were visualized using the Odyssey imaging system (Li-Cor Biosciences).

Pull-down and western blot analysis

Cell lysates were mixed with anti-GFP monoclonal antibody couple to agarose beads to enrich GFP tagged proteins according to the manufacturer's protocols (MBL, Nagoya, Japan). Pull-down lysates were separated by tris-glycine PAGE and transferred to nitrocellulose filters and visualized as previously described (18).

FRET analysis

Cells were transfected with the PICCHUx vector constructed to include the human CrkII protein and YFP and CFP on both ends of CrkII, plus an N-terminal CAAX motif (37). Three images were acquired for each set of measurements, as follows: YFP excitation/YFP emission image (YFP channel); CFP excitation/CFP emission image (CFP channel); and CFP excitation/YFP emission image (FRET channel). Single-labeled (CFP or YFP) cells were used to calculate the non-FRET fluorescence bleed-through produced by the fluorophores into the FRET channel, and the non-FRET fluorescent intensity values were subtracted from the apparent FRET intensities obtained from the double-labeled cells under the same conditions. A set of reference images was acquired from single-labeled CFP- or YFP-expressing cells for each set of acquisition parameters, and a calibration curve was derived to allow elimination of the non-FRET components from the FRET channel. The FRET efficiency was calculated on a pixel-by-pixel basis using ImageJ software version 1.48v (NIH; <http://imagej.nih.gov/ij>).

Flow cytometry

Jurkat T cells expressing GFP-CrkII, GFP-CrkII (Y221D) or the GFP-CrkII (Y221A) were stimulated with immobilized anti-CD3 antibody and recombinant ICAM-1 for 24 hours, fixed and CD69 plasma membrane expression levels were determined by anti-CD69 PE antibody (FACSCaliber II; BD).

Enzyme-linked immunosorbent assay

To determine the concentration of secreted IL-2 following stimulation, a human IL-2 ELISA kit (BioLegend) was used according to the manufacturer's protocols. Cells were stimulated with immobilized anti-CD3 antibody and recombinant ICAM-1 for 48 hours following supernatant collection (73).

SHP-1 and SHP-2 knockdown

Jurkat cells were infected with lenti viruses containing SHP-1 (NM_002831.5-1391s21c1), SHP-2 (NM_002834.3-1570s1c1), and scramble (SHC016) shRNA vectors (MOI of 2.5) (Mission; Sigma). Puromycin (2 µg/ml) resistant clones were selected after 72 hours. Protein expressions levels were determined by western blotting. For primary human T cells siRNA (Dharmacon SMARTpool) were introduced by nucleofection, and experiments were performed 48 hours later.

Static adhesion assay

T cell adhesion was performed as recently described (45). Cells expressing GFP-tagged constructs were stimulated with anti-CD3 antibody prior to plating on optical bottom 96-well plates (Corning) precoated with ICAM-1. Cells were incubated for 15 minutes, to allow for cells to settle, followed by removal of non-adherent cells by serial washes. The percentage of adherent cells was determined with a fluorescent plate reader (Synergy HT, BioTek).

Statistical analysis

Prism software (Version 6) was used for *t*-tests and ANOVA analysis.

References

1. J. E. Smith-Garvin, G. A. Koretzky, M. S. Jordan, T cell activation. *Annual review of immunology* **27**, 591-619 (2009).
2. R. J. Brownlie, R. Zamoyska, T cell receptor signalling networks: branched, diversified and bounded. *Nature reviews. Immunology* **13**, 257-269 (2013).
3. M. Tapia, A. Mor, Lymphocyte adhesion and autoimmunity. *Bulletin of the Hospital for Joint Disease* **72**, 148-153 (2014).
4. A. Mor, M. L. Dustin, M. R. Philips, Small GTPases and LFA-1 reciprocally modulate adhesion and signaling. *Immunological reviews* **218**, 114-125 (2007).
5. I. Azoulay-Alfaguter, M. Strazza, A. Pedoeem, A. Mor, The coreceptor programmed death 1 inhibits T-cell adhesion by regulating Rap1. *The Journal of allergy and clinical immunology* **135**, 564-567 (2015).
6. M. Strazza, I. Azoulay-Alfaguter, B. Dun, J. Baquero-Buitrago, A. Mor, CD28 inhibits T cell adhesion by recruiting CAPRI to the plasma membrane. *Journal of immunology* **194**, 2871-2877 (2015).
7. M. L. Dustin, T. A. Springer, Lymphocyte function-associated antigen-1 (LFA-1) interaction with intercellular adhesion molecule-1 (ICAM-1) is one of at least three mechanisms for lymphocyte adhesion to cultured endothelial cells. *The Journal of cell biology* **107**, 321-331 (1988).
8. K. Katagiri, M. Hattori, N. Minato, T. Kinashi, Rap1 functions as a key regulator of T-cell and antigen-presenting cell interactions and modulates T-cell responses. *Molecular and cellular biology* **22**, 1001-1015 (2002).
9. W. A. Comrie, A. Babich, J. K. Burkhardt, F-actin flow drives affinity maturation and spatial organization of LFA-1 at the immunological synapse. *The Journal of cell biology* **208**, 475-491 (2015).
10. M. R. Kooistra, N. Dube, J. L. Bos, Rap1: a key regulator in cell-cell junction formation. *Journal of cell science* **120**, 17-22 (2007).
11. E. Manevich-Mendelson, S. W. Feigelson, R. Pasvolsky, M. Aker, V. Grabovsky, Z. Shulman, S. S. Kilic, M. A. Rosenthal-Allieri, S. Ben-Dor, A. Mory, A. Bernard, M. Moser, A. Etzioni, R. Alon, Loss of Kindlin-3 in LAD-III eliminates LFA-1 but not VLA-4 adhesiveness developed under shear flow conditions. *Blood* **114**, 2344-2353 (2009).
12. T. Kinashi, M. Aker, M. Sokolovsky-Eisenberg, V. Grabovsky, C. Tanaka, R. Shamri, S. Feigelson, A. Etzioni, R. Alon, LAD-III, a leukocyte adhesion deficiency syndrome associated with defective Rap1 activation and impaired stabilization of integrin bonds. *Blood* **103**, 1033-1036 (2004).
13. M. Moser, B. Nieswandt, S. Ussar, M. Pozgajova, R. Fassler, Kindlin-3 is essential for integrin activation and platelet aggregation. *Nature medicine* **14**, 325-330 (2008).
14. K. Katagiri, A. Maeda, M. Shimonaka, T. Kinashi, RAPL, a Rap1-binding molecule that mediates Rap1-induced adhesion through spatial regulation of LFA-1. *Nature immunology* **4**, 741-748 (2003).
15. B. Boettner, L. Van Aelst, Control of cell adhesion dynamics by Rap1 signaling. *Current opinion in cell biology* **21**, 684-693 (2009).
16. V. Radha, A. Mitra, K. Dayma, K. Sasikumar, Signalling to actin: role of C3G, a multitasking guanine-nucleotide-exchange factor. *Bioscience reports* **31**, 231-244 (2011).
17. F. J. Zwartkruis, J. L. Bos, Ras and Rap1: two highly related small GTPases with distinct function. *Experimental cell research* **253**, 157-165 (1999).
18. A. Mor, J. P. Wynne, I. M. Ahearn, M. L. Dustin, G. Du, M. R. Philips, Phospholipase D1 regulates lymphocyte adhesion via upregulation of Rap1 at the plasma membrane. *Molecular and cellular biology* **29**, 3297-3306 (2009).

19. S. Gelkop, G. D. Gish, Y. Babichev, T. Pawson, N. Isakov, T cell activation-induced CrkII binding to the Zap70 protein tyrosine kinase is mediated by Lck-dependent phosphorylation of Zap70 tyrosine 315. *Journal of immunology* **175**, 8123-8132 (2005).
20. P. R. Nath, G. Dong, A. Braiman, N. Isakov, Immunophilins control T lymphocyte adhesion and migration by regulating CrkII binding to C3G. *Journal of immunology* **193**, 3966-3977 (2014).
21. A. Braiman, N. Isakov, The Role of Crk Adaptor Proteins in T-Cell Adhesion and Migration. *Frontiers in immunology* **6**, 509 (2015).
22. Y. Huang, F. Clarke, M. Karimi, N. H. Roy, E. K. Williamson, M. Okumura, K. Mochizuki, E. J. Chen, T. J. Park, G. F. Debes, Y. Zhang, T. Curran, T. Kambayashi, J. K. Burkhardt, CRK proteins selectively regulate T cell migration into inflamed tissues. *The Journal of clinical investigation* **125**, 1019-1032 (2015).
23. S. K. Bromley, W. R. Burack, K. G. Johnson, K. Somersalo, T. N. Sims, C. Sumen, M. M. Davis, A. S. Shaw, P. M. Allen, M. L. Dustin, The immunological synapse. *Annual review of immunology* **19**, 375-396 (2001).
24. M. L. Dustin, The immunological synapse. *Cancer immunology research* **2**, 1023-1033 (2014).
25. T. G. Bivona, H. H. Wiener, I. M. Ahearn, J. Silletti, V. K. Chiu, M. R. Philips, Rap1 up-regulation and activation on plasma membrane regulates T cell adhesion. *The Journal of cell biology* **164**, 461-470 (2004).
26. M. Cote, C. Fos, A. J. Canonigo-Balancio, K. Ley, S. Becart, A. Altman, SLAT promotes TCR-mediated, Rap1-dependent LFA-1 activation and adhesion through interaction of its PH domain with Rap1. *Journal of cell science* **128**, 4341-4352 (2015).
27. J. P. Wynne, J. Wu, W. Su, A. Mor, N. Patsoukis, V. A. Boussiotis, S. R. Hubbard, M. R. Philips, Rap1-interacting adapter molecule (RIAM) associates with the plasma membrane via a proximity detector. *The Journal of cell biology* **199**, 317-330.
28. M. C. Seabra, Membrane association and targeting of prenylated Ras-like GTPases. *Cellular signalling* **10**, 167-172 (1998).
29. C. L. Williams, The polybasic region of Ras and Rho family small GTPases: a regulator of protein interactions and membrane association and a site of nuclear localization signal sequences. *Cellular signalling* **15**, 1071-1080 (2003).
30. I. Azoulay-Alfaguter, M. Strazza, A. Mor, Chaperone-mediated specificity in Ras and Rap signaling. *Critical reviews in biochemistry and molecular biology* **50**, 194-202 (2015).
31. J. A. Gorman, A. Babich, C. J. Dick, R. A. Schoon, A. Koenig, T. S. Gomez, J. K. Burkhardt, D. D. Billadeau, The cytoskeletal adaptor protein IQGAP1 regulates TCR-mediated signaling and filamentous actin dynamics. *Journal of immunology* **188**, 6135-6144 (2012).
32. S. Yamashita, N. Mochizuki, Y. Ohba, M. Tobiume, Y. Okada, H. Sawa, K. Nagashima, M. Matsuda, CalDAG-GEFIII activation of Ras, R-ras, and Rap1. *The Journal of biological chemistry* **275**, 25488-25493 (2000).
33. S. Sawasdikosol, K. S. Ravichandran, K. K. Lee, J. H. Chang, S. J. Burakoff, Crk interacts with tyrosine-phosphorylated p116 upon T cell activation. *The Journal of biological chemistry* **270**, 2893-2896 (1995).
34. K. A. Reedquist, T. Fukazawa, G. Panchamoorthy, W. Y. Langdon, S. E. Shoelson, B. J. Druker, H. Band, Stimulation through the T cell receptor induces Cbl association with Crk proteins and the guanine nucleotide exchange protein C3G. *The Journal of biological chemistry* **271**, 8435-8442 (1996).
35. D. Liu, The adaptor protein Crk in immune response. *Immunology and cell biology* **92**, 80-89 (2014).

36. G. Huyer, S. Liu, J. Kelly, J. Moffat, P. Payette, B. Kennedy, G. Tsaprailis, M. J. Gresser, C. Ramachandran, Mechanism of inhibition of protein-tyrosine phosphatases by vanadate and pervanadate. *The Journal of biological chemistry* **272**, 843-851 (1997).
37. K. Kurokawa, N. Mochizuki, Y. Ohba, H. Mizuno, A. Miyawaki, M. Matsuda, A pair of fluorescent resonance energy transfer-based probes for tyrosine phosphorylation of the CrkII adaptor protein in vivo. *The Journal of biological chemistry* **276**, 31305-31310 (2001).
38. A. Mor, G. Campi, G. Du, Y. Zheng, D. A. Foster, M. L. Dustin, M. R. Philips, The lymphocyte function-associated antigen-1 receptor costimulates plasma membrane Ras via phospholipase D2. *Nature cell biology* **9**, 713-719 (2007).
39. D. K. Sojka, D. Bruniquel, R. H. Schwartz, N. J. Singh, IL-2 secretion by CD4+ T cells in vivo is rapid, transient, and influenced by TCR-specific competition. *Journal of immunology* **172**, 6136-6143 (2004).
40. J. C. Nolz, L. P. Nacusi, C. M. Segovis, R. B. Medeiros, J. S. Mitchell, Y. Shimizu, D. D. Billadeau, The WAVE2 complex regulates T cell receptor signaling to integrins via Abl- and CrkL-C3G-mediated activation of Rap1. *The Journal of cell biology* **182**, 1231-1244 (2008).
41. L. Chen, S. S. Sung, M. L. Yip, H. R. Lawrence, Y. Ren, W. C. Guida, S. M. Sebt, N. J. Lawrence, J. Wu, Discovery of a novel shp2 protein tyrosine phosphatase inhibitor. *Molecular pharmacology* **70**, 562-570 (2006).
42. Y. M. Li, J. E. Casida, Cantharidin-binding protein: identification as protein phosphatase 2A. *Proceedings of the National Academy of Sciences of the United States of America* **89**, 11867-11870 (1992).
43. S. M. Stanford, N. Rapini, N. Bottini, Regulation of TCR signalling by tyrosine phosphatases: from immune homeostasis to autoimmunity. *Immunology* **137**, 1-19 (2012).
44. Z. Z. Chong, K. Maiese, The Src homology 2 domain tyrosine phosphatases SHP-1 and SHP-2: diversified control of cell growth, inflammation, and injury. *Histology and histopathology* **22**, 1251-1267 (2007).
45. M. Strazza, I. Azoulay-Alfaguter, A. Pedoeem, A. Mor, Static adhesion assay for the study of integrin activation in T lymphocytes. *Journal of visualized experiments : JoVE*, (2014).
46. H. Schneider, J. Downey, A. Smith, B. H. Zinselmeyer, C. Rush, J. M. Brewer, B. Wei, N. Hogg, P. Garside, C. E. Rudd, Reversal of the TCR stop signal by CTLA-4. *Science* **313**, 1972-1975 (2006).
47. T. Gotoh, S. Hattori, S. Nakamura, H. Kitayama, M. Noda, Y. Takai, K. Kaibuchi, H. Matsui, O. Hatase, H. Takahashi, et al., Identification of Rap1 as a target for the Crk SH3 domain-binding guanine nucleotide-releasing factor C3G. *Molecular and cellular biology* **15**, 6746-6753 (1995).
48. R. B. Birge, C. Kalodimos, F. Inagaki, S. Tanaka, Crk and CrkL adaptor proteins: networks for physiological and pathological signaling. *Cell communication and signaling : CCS* **7**, 13 (2009).
49. Y. Ohashi, K. Tachibana, K. Kamiguchi, H. Fujita, C. Morimoto, T cell receptor-mediated tyrosine phosphorylation of Cas-L, a 105-kDa Crk-associated substrate-related protein, and its association of Crk and C3G. *The Journal of biological chemistry* **273**, 6446-6451 (1998).
50. G. Campi, R. Varma, M. L. Dustin, Actin and agonist MHC-peptide complex-dependent T cell receptor microclusters as scaffolds for signaling. *The Journal of experimental medicine* **202**, 1031-1036 (2005).
51. D. D. Billadeau, T cell activation at the immunological synapse: vesicles emerge for LATer signaling. *Science signaling* **3**, pe16 (2010).

52. M. A. Purbhoo, H. Liu, S. Oddos, D. M. Owen, M. A. Neil, S. V. Pagoon, P. M. French, C. E. Rudd, D. M. Davis, Dynamics of subsynaptic vesicles and surface microclusters at the immunological synapse. *Science signaling* **3**, ra36 (2010).
53. A. Mor, M. R. Philips, Compartmentalized Ras/MAPK signaling. *Annual review of immunology* **24**, 771-800 (2006).
54. P. Sarkar, C. Reichman, T. Saleh, R. B. Birge, C. G. Kalodimos, Proline cis-trans isomerization controls autoinhibition of a signaling protein. *Molecular cell* **25**, 413-426 (2007).
55. P. Sarkar, T. Saleh, S. R. Tzeng, R. B. Birge, C. G. Kalodimos, Structural basis for regulation of the Crk signaling protein by a proline switch. *Nature chemical biology* **7**, 51-57 (2011).
56. P. R. Nath, N. Isakov, Insights into peptidyl-prolyl cis-trans isomerase structure and function in immunocytes. *Immunology letters* **163**, 120-131 (2015).
57. P. R. Nath, G. Dong, A. Braiman, N. Isakov, In vivo regulation of human CrkII by cyclophilin A and FK506-binding protein. *Biochemical and biophysical research communications* **470**, 411-416 (2016).
58. S. Kumari, S. Vardhana, M. Cammer, S. Curado, L. Santos, M. P. Sheetz, M. L. Dustin, T Lymphocyte Myosin IIA is Required for Maturation of the Immunological Synapse. *Frontiers in immunology* **3**, 230 (2012).
59. K. Choudhuri, J. Llodra, E. W. Roth, J. Tsai, S. Gordo, K. W. Wucherpennig, L. C. Kam, D. L. Stokes, M. L. Dustin, Polarized release of T-cell-receptor-enriched microvesicles at the immunological synapse. *Nature* **507**, 118-123 (2014).
60. Y. Yarden, A. Ullrich, Growth factor receptor tyrosine kinases. *Annual review of biochemistry* **57**, 443-478 (1988).
61. T. Hunter, Protein modification: phosphorylation on tyrosine residues. *Current opinion in cell biology* **1**, 1168-1181 (1989).
62. J. Kwon, C. K. Qu, J. S. Maeng, R. Falahati, C. Lee, M. S. Williams, Receptor-stimulated oxidation of SHP-2 promotes T-cell adhesion through SLP-76-ADAP. *The EMBO journal* **24**, 2331-2341 (2005).
63. Y. Yu, A. A. Smoligovets, J. T. Groves, Modulation of T cell signaling by the actin cytoskeleton. *Journal of cell science* **126**, 1049-1058 (2013).
64. M. L. Dustin, J. T. Groves, Receptor signaling clusters in the immune synapse. *Annual review of biophysics* **41**, 543-556 (2012).
65. D. A. Dehring, F. Clarke, B. G. Ricart, Y. Huang, T. S. Gomez, E. K. Williamson, D. A. Hammer, D. D. Billadeau, Y. Argon, J. K. Burkhardt, Hematopoietic lineage cell-specific protein 1 functions in concert with the Wiskott-Aldrich syndrome protein to promote podosome array organization and chemotaxis in dendritic cells. *Journal of immunology* **186**, 4805-4818 (2011).
66. Y. Sasahara, R. Rachid, M. J. Byrne, M. A. de la Fuente, R. T. Abraham, N. Ramesh, R. S. Geha, Mechanism of recruitment of WASP to the immunological synapse and of its activation following TCR ligation. *Molecular cell* **10**, 1269-1281 (2002).
67. M. Raab, X. Smith, Y. Matthes, K. Strebhardt, C. E. Rudd, SKAP1 protein PH domain determines RapL membrane localization and Rap1 protein complex formation for T cell receptor (TCR) activation of LFA-1. *The Journal of biological chemistry* **286**, 29663-29670 (2011).
68. M. Raab, H. Wang, Y. Lu, X. Smith, Z. Wu, K. Strebhardt, J. E. Ladbury, C. E. Rudd, T cell receptor "inside-out" pathway via signaling module SKAP1-RapL regulates T cell motility and interactions in lymph nodes. *Immunity* **32**, 541-556 (2010).
69. W. Su, J. Wynne, E. M. Pinheiro, M. Strazza, A. Mor, E. Montenont, J. Berger, D. S. Paul, W. Bergmeier, F. B. Gertler, M. R. Philips, Rap1 and its effector RIAM are required for lymphocyte trafficking. *Blood* **126**, 2695-2703 (2015).

70. E. Choy, V. K. Chiu, J. Silletti, M. Feoktistov, T. Morimoto, D. Michaelson, I. E. Ivanov, M. R. Philips, Endomembrane trafficking of ras: the CAAX motif targets proteins to the ER and Golgi. *Cell* **98**, 69-80 (1999).
71. Y. Kloog, A. Mor, Cytotoxic-T-lymphocyte antigen 4 receptor signaling for lymphocyte adhesion is mediated by C3G and Rap1. *Molecular and cellular biology* **34**, 978-988 (2014).
72. R. Varma, G. Campi, T. Yokosuka, T. Saito, M. L. Dustin, T cell receptor-proximal signals are sustained in peripheral microclusters and terminated in the central supramolecular activation cluster. *Immunity* **25**, 117-127 (2006).
73. A. Zanin-Zhorov, J. M. Weiss, M. S. Nyuydzefe, W. Chen, J. U. Scher, R. Mo, D. Depoil, N. Rao, B. Liu, J. Wei, S. Lucas, M. Koslow, M. Roche, O. Schueller, S. Weiss, M. V. Poyurovsky, J. Tonra, K. L. Hippen, M. L. Dustin, B. R. Blazar, C. J. Liu, S. D. Waksal, Selective oral ROCK2 inhibitor down-regulates IL-21 and IL-17 secretion in human T cells via STAT3-dependent mechanism. *Proceedings of the National Academy of Sciences of the United States of America* **111**, 16814-16819 (2014).

Acknowledgments

We thank Mark Philips (NYU) for helpful discussions, David Depoil (NYU) and Michael Cammer (NYU) for their assistance with TIRF microscope, Philip Stork (The Vollum Institute) for providing the C3G-GFP vector, Kenneth Yamada (NIH) for providing the GFP-CrkII vector, Lynda Chin (Harvard Medical School) for the flag-CasL-HA plasmid, Michiyuki Matsuda (Osaka University) for offering the PICCHUx vector and Ben Neel (NYU) for the SHP-1-MSCV-IRES-GFP plasmid. This work was supported by NIH grants AI043542 (M.L.D.) and R01AI125640 (A.M.), Irma T. Hirschl Trust (A.M.), The Colton Family (A.M.), and the Rheumatology Research Foundation (A.M.).

Author contributions: I.A. and A.M. planned the experiments. I.A. and A.M. performed the experiments. I.A., M.S. and M.P. analyzed the data and provided comments. H.N. and J.M. for their assistance and support with the SLB experiments.. M.L.D. contributed to design and interpretation of SLB experiments. I.A. and A.M. wrote the paper.

The authors declare no conflict of interest.

Figure legends

Figure 1. T cell receptor signaling to adhesion. Major signaling proteins downstream of the T cell receptor (TCR) leading to Rap1 activation and LFA-1 mediated adhesion are shown.

Figure 2. Activated Rap1 is recruited to the immunological synapse. (A) Jurkat T cells were co-transfected with GFP-RalGDS-RBD (the probe for activated Rap1) and Cherry-Rap1, co-cultured with Raji B cells (APC) preloaded with SEE (1.5 $\mu\text{g/ml}$), and imaged alive. (B) OT-II T cells were co-transfected with GFP-RalGDS-RBD and Cherry-Rap1, cocultured with dendritic cells (DC) pulsed with 100 $\mu\text{g/ml}$ OVA peptide and imaged alive. (C) Primary human T cells were transfected with GFP tagged -Rap1, -N-Ras, -RalGDS-RBD, or -Raf1-RBD (the probe for activated Ras) and introduced onto supported lipid bilayers containing anti-CD3 antibody (5 $\mu\text{g/ml}$) labeled with Alexa Fluor 568 and ICAM-1 (250 molecules/ mm^2) tagged with Alexa Fluor 405. Live cells were imaged with TIRF microscopy at different time points. (D, E) Quantification of the distribution of different proteins within the compartments of the IS at 20 minutes (* $P < 0.05$, $n > 3$, at least 50 cells in each experiment, scale bar is 10 μm). (F) Schematic of the different compartments of the immunological synapse.

Figure 3. What are the factors regulating Rap1 localization in the immunological synapse?

(A) Primary human T cells expressing GFP tagged-Rap1 (wild type), -Rap1 CVVM (Rap1 with N-Ras tail), -Rap1V12 (GTP loaded Rap1), -Rap1N17 (GDP loaded Rap1), -C3G, -C3G Y504D (phosphomimetic), or -CalDAG-GEFIII, were introduced onto supported lipid bilayers containing anti-CD3 (5 $\mu\text{g/ml}$) labeled with Alexa Fluor 568 and ICAM-1 (250 molecules/ mm^2) tagged with Alexa Fluor 405 and imaged alive by TIRF microscopy at multiple time points. (B, C, D) Quantification of the distribution of the different GFP tagged proteins within different

compartments of the immunological synapse at 20 minutes (* $P < 0.05$, $n > 3$, at least 50 cells were counted in each experiment, scale bar is 10 μm).

Figure 4. CrkII localization in the immunological synapse is regulated by phosphorylation.

(A) Domains structure of active (dephosphorylated) vs. inactive (phosphorylated) CrkII. (B) Primary human T cells were transfected with GFP labeled wild type CrkII, phosphodeficient CrkII (Y221A), or phosphomimetic CrkII (Y221D), introduced onto supported lipid bilayers containing fluorescently labeled anti-CD3 antibody (5 $\mu\text{g/ml}$) and ICAM-1 (250 molecules/ mm^2) and imaged alive at different time points. (C) Quantification of the relative distribution of the different versions of CrkII in the IS ($n=3$, at least 50 cells were counted in each experiment, * $P < 0.05$, NS; not significant). (D) Primary human T cells expressing GFP-CrkII were plated on supported lipid bilayers containing fluorescently labeled anti-CD3 antibody (5 $\mu\text{g/ml}$) and ICAM-1 (250 molecules/ mm^2), treated with pervanadate (50 μM) and imaged alive. (E) Quantification of the relative distribution of CrkII, before and after treatment with pervanadate within the different compartments of the IS ($n=3$, more than 25 cells were counted in each experiment).

Figure 5. CrkII dephosphorylation regulates T cell activation.

(A) Jurkat T cells were stimulated with 5 $\mu\text{g/ml}$ of anti-CD3 antibody for 2 to 5 minutes, lysed and loaded on SDS-PAGE gel. CrkII phosphorylation levels were analyzed by western blot using anti-CrkII and anti-pCrkII specific antibody. (B) Quantification of the ratio between phosphorylated CrkII and total CrkII after stimulation with anti-CD3 antibody (5 $\mu\text{g/ml}$) ($n=3$, ** $P < 0.05$, *** $P < 0.001$). (C) Jurkat T cells expressing the PICCHUx construct (YFP-CrkII-CFP-CAAX) were treated with anti-CD3 antibody (5 $\mu\text{g/ml}$), fixed with 2% PFA and FRET emission was recorded (excitation at 433 nm, emission 530 nm) (scale bar is 10 μm). (D) Bars represent quantification of FRET efficiency ($n=3$, **** $P < 0.0001$). (E) Jurkat T cells expressing GFP labeled-CrkII (wild type), -CrkII

Y221A, or -CrkII Y221D were stimulated with anti-CD3 antibody (5 μ g/ml) and levels of activated Rap1 were measured by GST-pull assay (n=3, * P <0.05). (F) Jurkat T cells expressing GFP labeled-CrkII (wild type), -CrkII Y221A, or -CrkII Y221D were stimulated with anti-CD3 antibody (5 μ g/ml) and adhesion to ICAM-1 coated wells was recorded. (G) Jurkat T cells expressing GFP-CrkII, -CrkII Y221A, or -CrkII Y221A were stimulated with anti-CD3 antibody (1 μ g/ml), plated over night on ICAM-1 (2 μ g/mL) coated wells and CD69 expression levels were measured by flow cytometer. (H) Jurkat T cells expressing either GFP-CrkII, -CrkII Y221A, or -CrkII Y221D were stimulated with anti-CD3 antibody (1 μ g/ml), plated on ICAM-1 (2 μ g/ml) coated wells and levels of supernatant IL-2 after 48 hours were measured (n=3, ** P < 0.01, NS; not significant).

Figure 6. SHP-1 dephosphorylates CrkII downstream of the T cell receptor. (A) Jurkat T cells expressing GFP-CrkII were pre-treated with either SHP-1/2 inhibitor (NSC-878771; 20 mM for 30 minutes) or with PP2A inhibitor (Cantharidic acid; 400 mM for 30 minutes), stimulated with anti-CD3 antibody (5 μ g/ml) for 2 minutes, lysed and levels of CrkII phosphorylation were measured by western blot. Relative levels of phosphorylated CrkII over total CrkII are shown (n=3). (B) Jurkat T cells expressing GFP or GFP-CrkII Y221A were pre-treated with NSC-87877 (as described earlier) prior to stimulation with anti-CD3 antibody (1 μ g/ml) and plating on ICAM-1 coated wells. Percentage of adherent cells was recorded after 15 minutes (n=3, ** P < 0.01, **** P <0.0001). (C) Jurkat T cells were infected with lentiviruses carrying scrambled, SHP-1, or SHP-2 targeted shRNA. Levels of SHP-1 and SHP-2 recorded after 48 hours. (D) Jurkat T cells expressing GFP-CrkII and the relevant shRNA were treated with anti-CD3 antibody (5 μ g/ml) for 5 minutes. Cell lysates were immunoprecipitated using anti-GFP antibodies and immunoblotted with anti-p-Tyr antibody. (E) Quantification of three experiments is shown (* P <0.05). (F-G) Jurkat T cells expressing scrambled, SHP-1, or SHP-2 targeted

shRNA (F), or primary human T cells treated with control, SHP-1 or SHP-2 siRNA (G) were treated with anti-CD3 antibody (5 μ g/ml) and adhesion to ICAM-1 coated wells was measured (n=3, $**P < 0.01$, NS; not significant). (H) SHP-1 was either knocked down with shRNA (SHP1-KD) in Jurkat T cells expressing untagged GFP, or rescued by overexpressing alternative SHP-1 construct (GFP-SHP-1) were treated with anti-CD3 antibody (5 μ g/ml) and adhesion to ICAM-1 coated wells was measured (n=3, $**P < 0.01$). (I) Primary human T cells treated with SHP-1 or SHP-2 siRNA were stimulated with soluble anti-CD3 antibody (5 μ g/ml) and assessed for motility on ICAM-1 coated plates. (J) Jurkat T cells expressing GFP-RalGDS-RBD and either shSHP-1 or shSHP-2 constructs were cocultured with Raji B cells preloaded with SEE (1.5 μ g/ml) and imaged alive. (K) Primary human T cells were treated with the relevant siRNA, cocultured with SEE preloaded Raji B cells and percentages of transient vs. stable conjugates were recorded. (L) Primary human T cells expressing GFP-RalGDS-RBD treated with the indicated siRNA were cocultured with SEE preloaded Raji B cells and imaged alive. Percentage of predominant phenotype is shown (n=4).

Figure 7. Model for CrkII location and function in the immunological synapse. TCR ligation leads to SHP-1 mediated CrkII dephosphorylation. Dephosphorylated CrkII travels from the c-SMAC to p-SMAC where it binds to the exchange factor C3G. C3G directly activates Rap1 leading to LFA-1 activation and enhanced T cell adhesion.

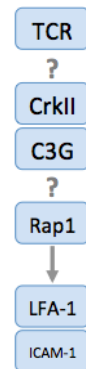


Figure 1. *T cell receptor signaling to adhesion.*

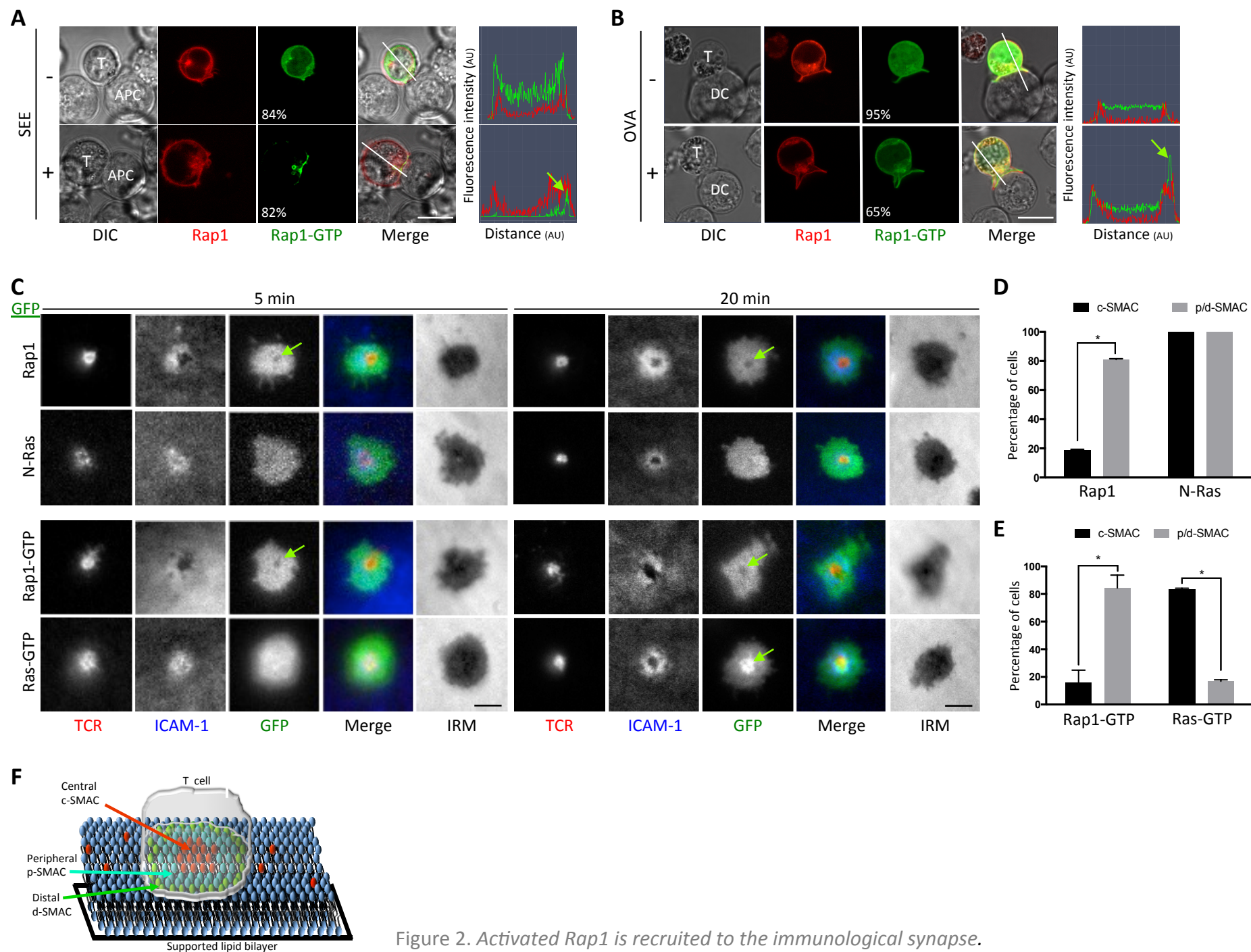


Figure 2. Activated *Rap1* is recruited to the immunological synapse.

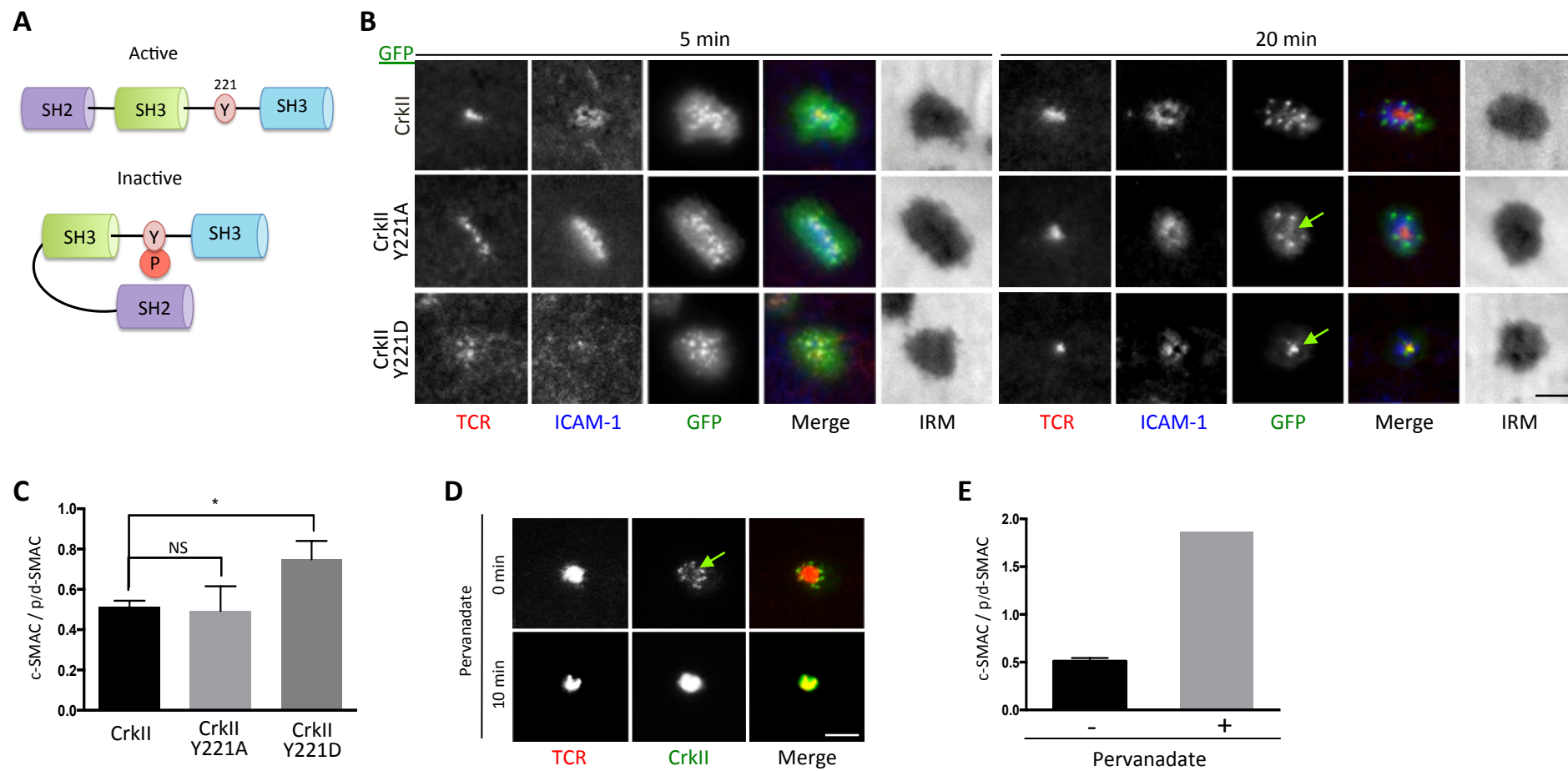


Figure 4. *CrkII* localization in the immunological synapse is regulated by phosphorylation.

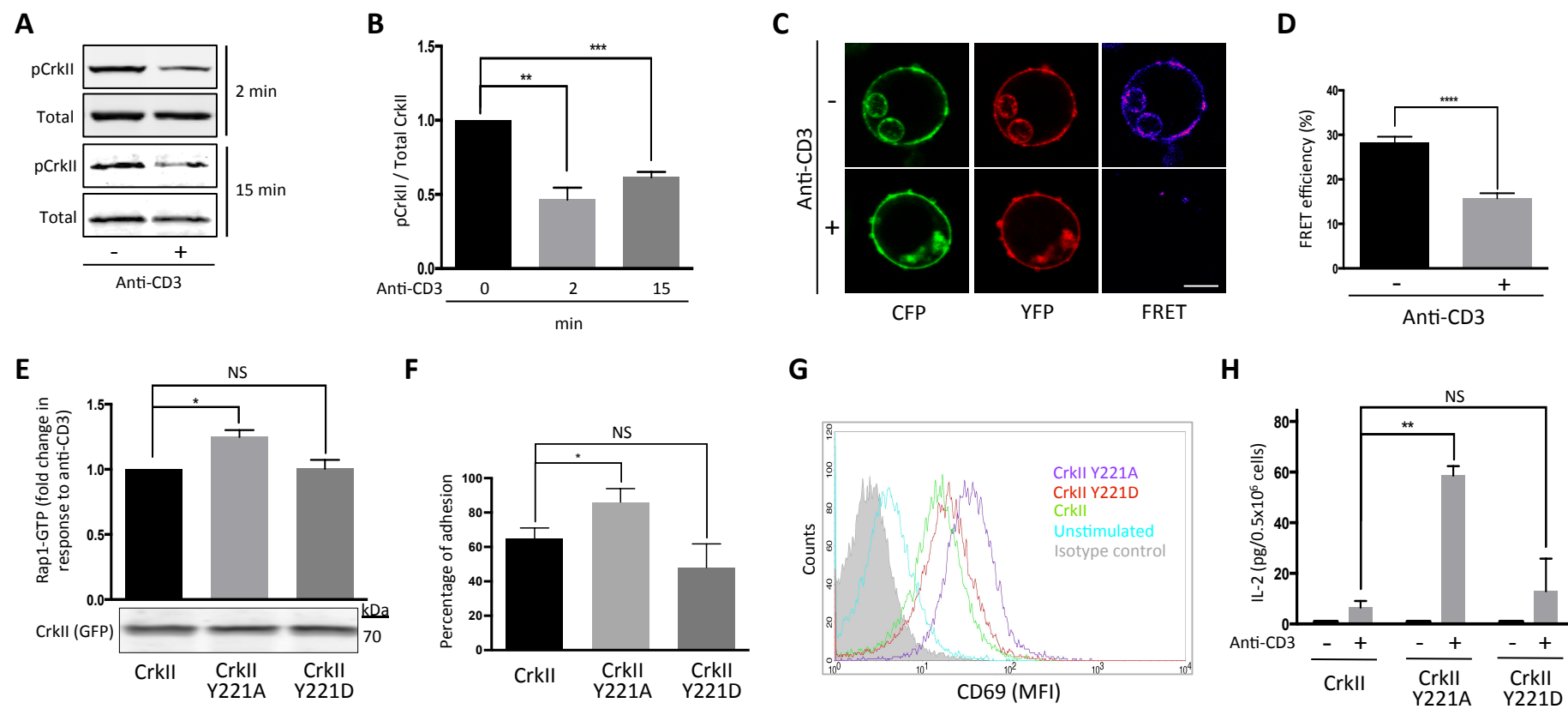


Figure 5. *CrkII* dephosphorylation regulates *T* cell activation.

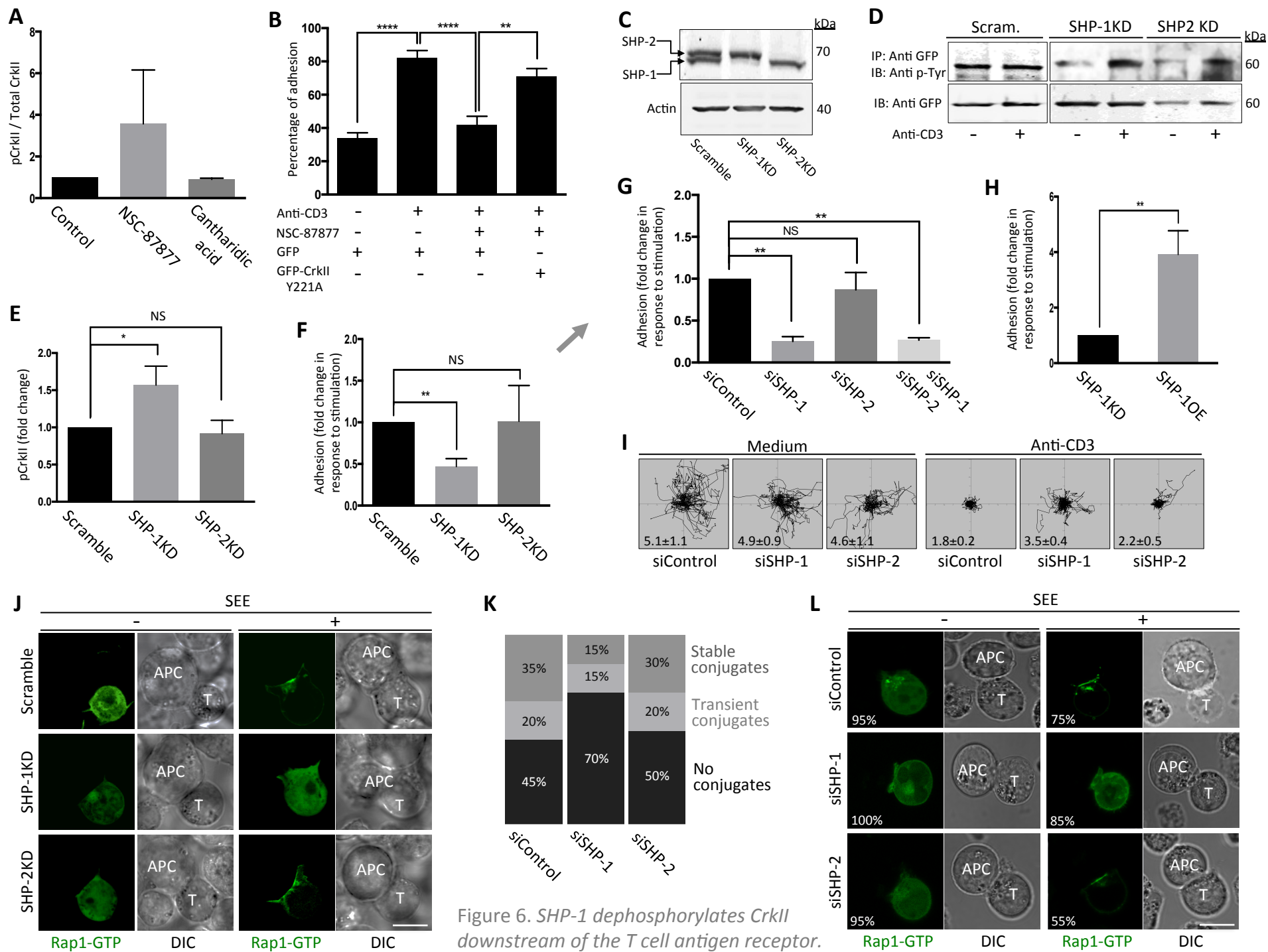


Figure 6. *SHP-1* dephosphorylates *CrklI* downstream of the T cell antigen receptor.

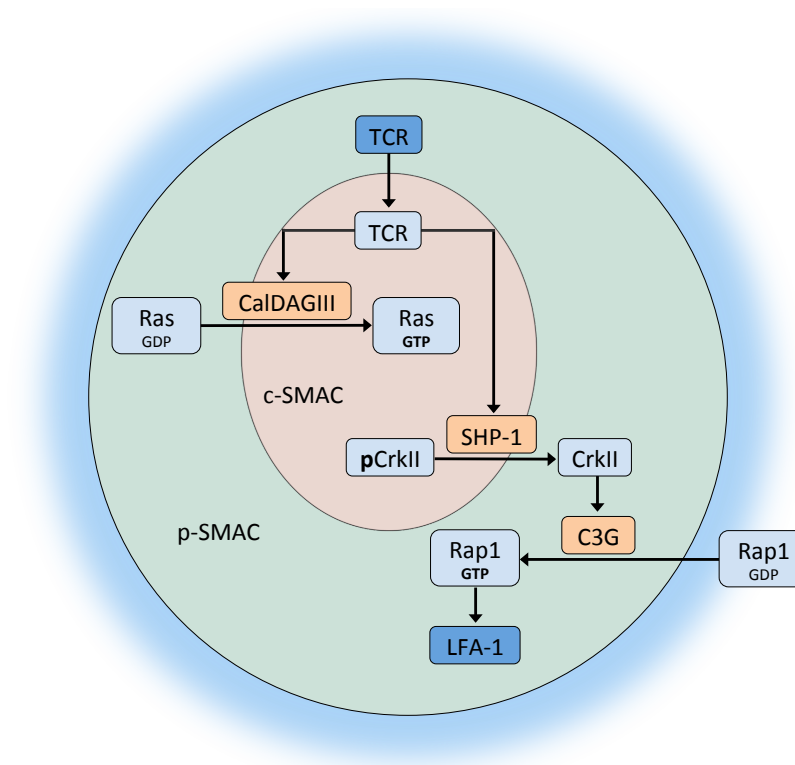


Figure 7. Model for CrkII location and function in the immunological synapse.

Supplementary materials

Fig. S1: Conjugates formation between Jurkat and SEE pulsed Raji cells.

Fig. S2: GFP-CAAX is not excluded from the c-SMAC.

Fig. S3: The hyper variable tail of Rap1 was replaced with N-Ras tail.

Fig. S4: Expression levels of GFP-Rap1V12 and GFP-Rap1N17.

Fig. S5: CrkII interacts with both C3G and CasL.

Fig. S6: Pervanadate treatment results in phosphorylation of CrkII at position 221.

Fig. S7: Stimulation via the T cell receptor leads to recruitment of CrkII to the membranous fraction.

Fig. S8: PicchuX-Y221D construct is folded prior to stimulation.

Figure S1. Conjugates formation between Jurkat and SEE pulsed Raji cells. Jurkat T cells were transfected with GFP-RalGDS-RBD, cultured with Raji B cells preloaded with SEE, and the percentage of transient and stable conjugates were recorded according to classification that has been previously reported (4, 5).

Figure S2. GFP-CAAX is not excluded from the c-SMAC. Primary human T cells were transfected with GFP-CAAX and were plated on supported lipid bilayers containing fluorescently labeled anti-CD3 antibodies and ICAM-1 and imaged alive.

Figure S3. The hyper variable tail of Rap1 was replaced with N-Ras tail. Schematic presentation of Rap1 and N-Ras lipid tails.

Figure S4. Expression levels of GFP-Rap1V12 and GFP-Rap1N17. Jurkat T cells transfected with Rap1V12 (GTP loaded Rap1) or Rap1N17 (GDP loaded Rap1) were subjected to western blot analysis to evaluate expression levels.

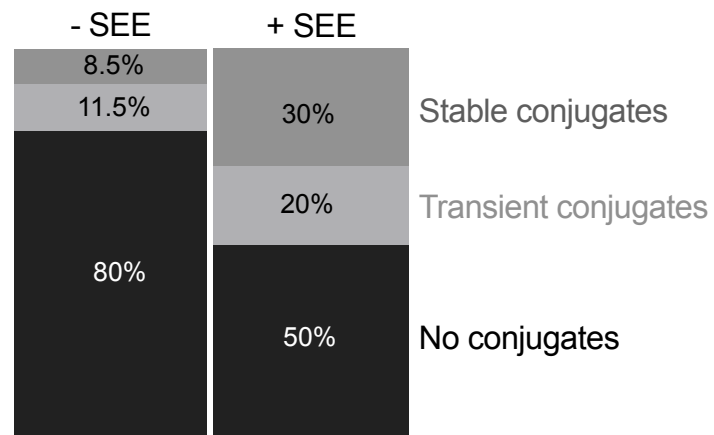
Figure S5. CrkII interacts with both C3G and CasL. (A) Jurkat T cells expressing GFP (negative control), GFP-CrkII Y221A (positive control), or GFP-CrkII (wild type) were treated with of anti-CD3 antibodies (5 μ g/ml), lysed and immunoprecipitated with anti-GFP antibodies. Endogenous C3G levels were analyzed with anti-C3G antibodies (Representative blot of three experiments is shown). (B) Blots were quantified and fold change in GFP-CrkII binding to C3G are shown (n = 3, * $P < 0.05$). (C) 293T cells were transfected with CasL-HA, and either GFP or GFP-CrkII. Cells were harvested 48 hours after transfection, immunoprecipitated with anti-GFP antibodies, and immunoblotted with anti-HA antibodies (Representative of three independent

experiments is shown). (D) Blots were quantified and fold change of GFP-CrkII binding to CasL are shown ($n = 3$, **** $P < 0.0001$).

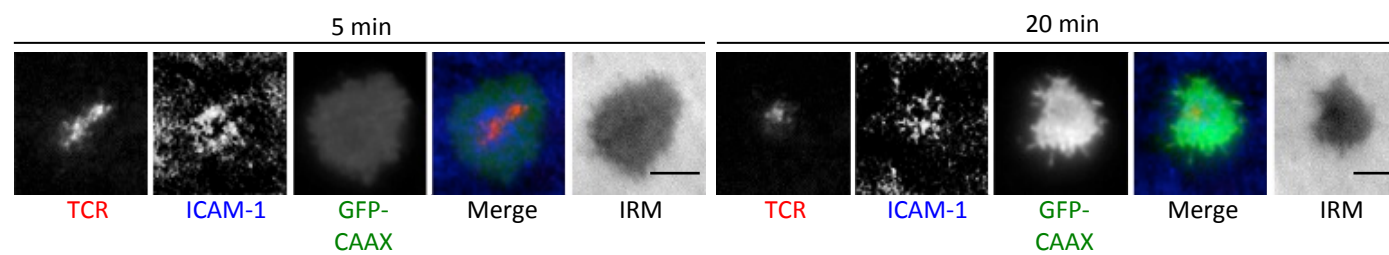
Figure S6. Pervanadate treatment results in phosphorylation of CrkII at position 221. (A) Jurkat T cell were treated with pervanadate (50 μ M) for 10 minutes and then blotted with pCrkII Tyr221 specific antibodies. (B) Quantification of the same experiment.

Figure S7. Stimulation via the T cell receptor leads to recruitment of CrkII to the membranous fraction. (A) Jurkat T cells were stimulated with 5 μ g/ml of anti-CD3 antibodies, lysed with nonident buffer, and separated to cellular vs. membranous fraction by centrifugation at 100,000xg for 45 minutes. CrkII levels were analyzed by western blot using anti-CrkII 3 antibodies. (B) Quantification of the same experiment showing fold change in membranous CrkII ($n = 2$, ** $P < 0.01$).

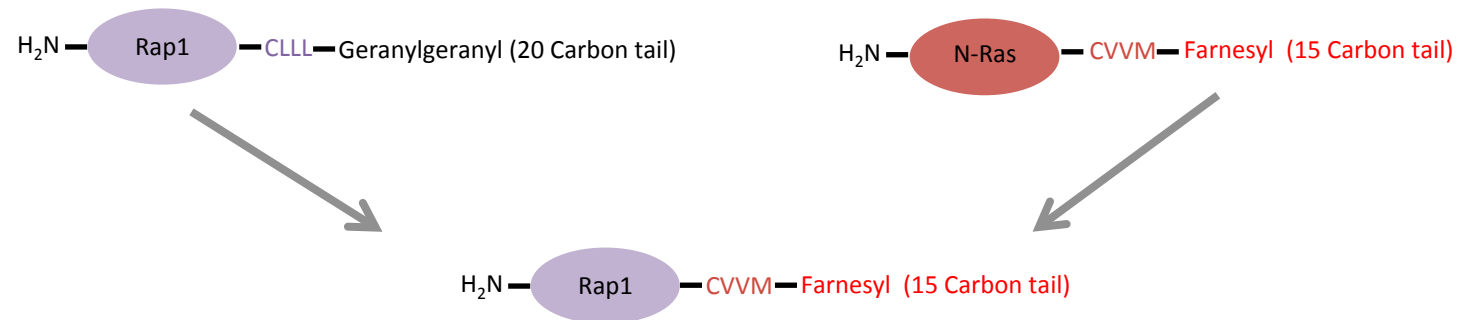
Figure S8. PicchuX-Y221D construct is folded prior to stimulation. (A, B) Jurkat T cells expressing the PICCHUxY221D vector (YFP-CrkIly221D-CFP-CAAX) (A) or the PICCHUxY221A vector (YFP-CrkIly221A-CFP-CAAX) were treated with anti-CD3 antibodies (5 μ g/ml), fixed with 2% PFA and FRET emission was recorded (excitation at 433nm, emission 530nm, scale bar is 10 μ m). (C) Bars represent quantification of FRET efficiency ($n = 3$).



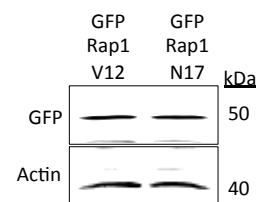
Supplementary Figure 1. *Conjugates formation between Jurkat and SEE pulsed Raji cells.*



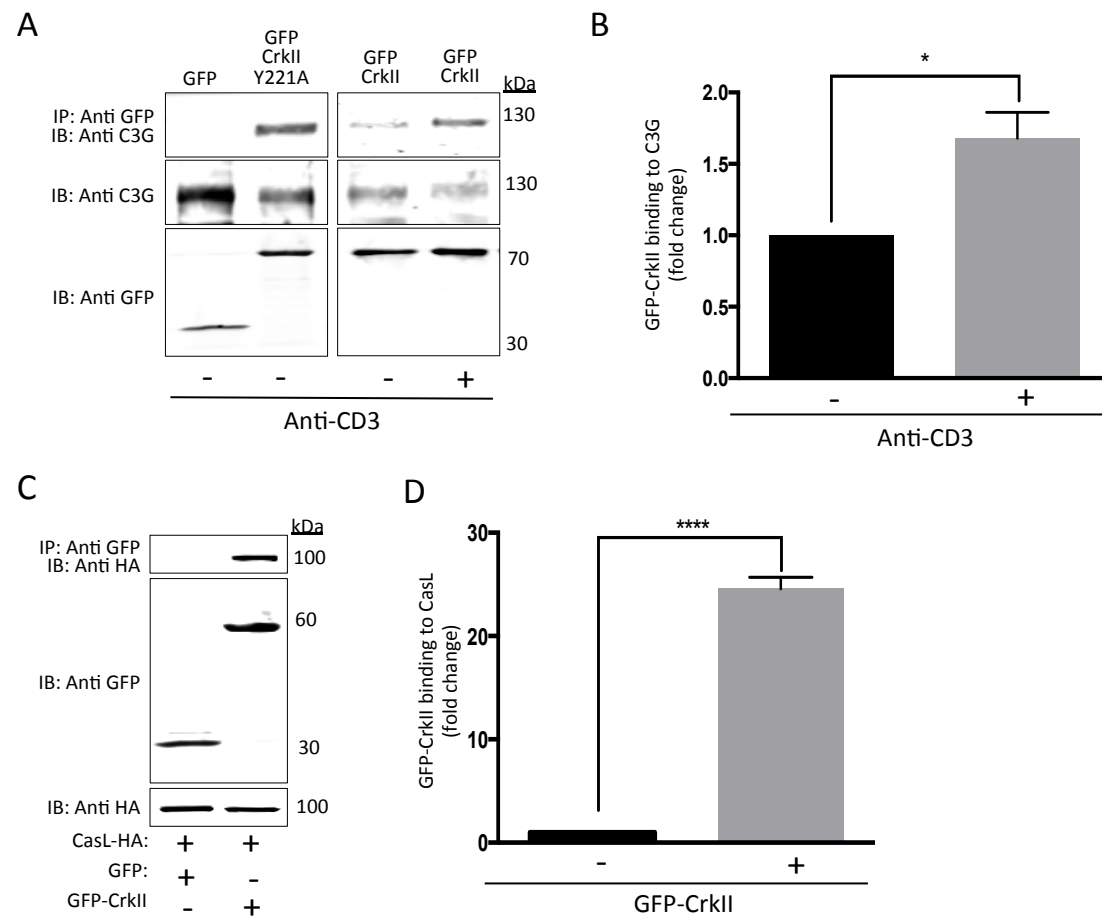
Supplementary Figure 2. *GFP-CAAX is not excluded from the c-SMAC.*



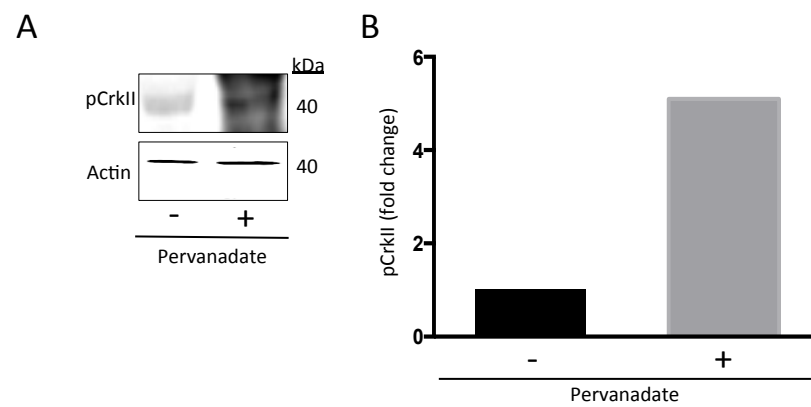
Supplementary Figure 3. *The hyper variable tail of Rap1 was replaced with N-Ras tail.*



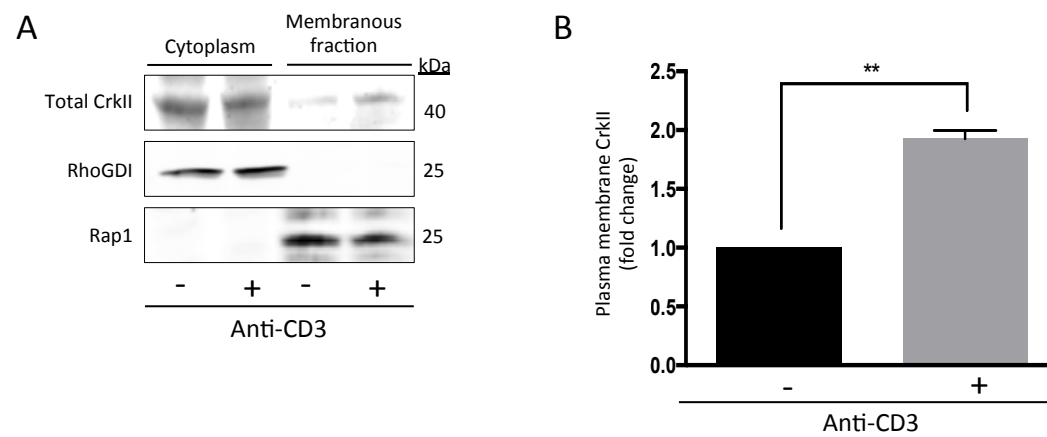
Supplementary Figure 4. *Expression levels of GFP-Rap1V12 and GFP-Rap1N17.*



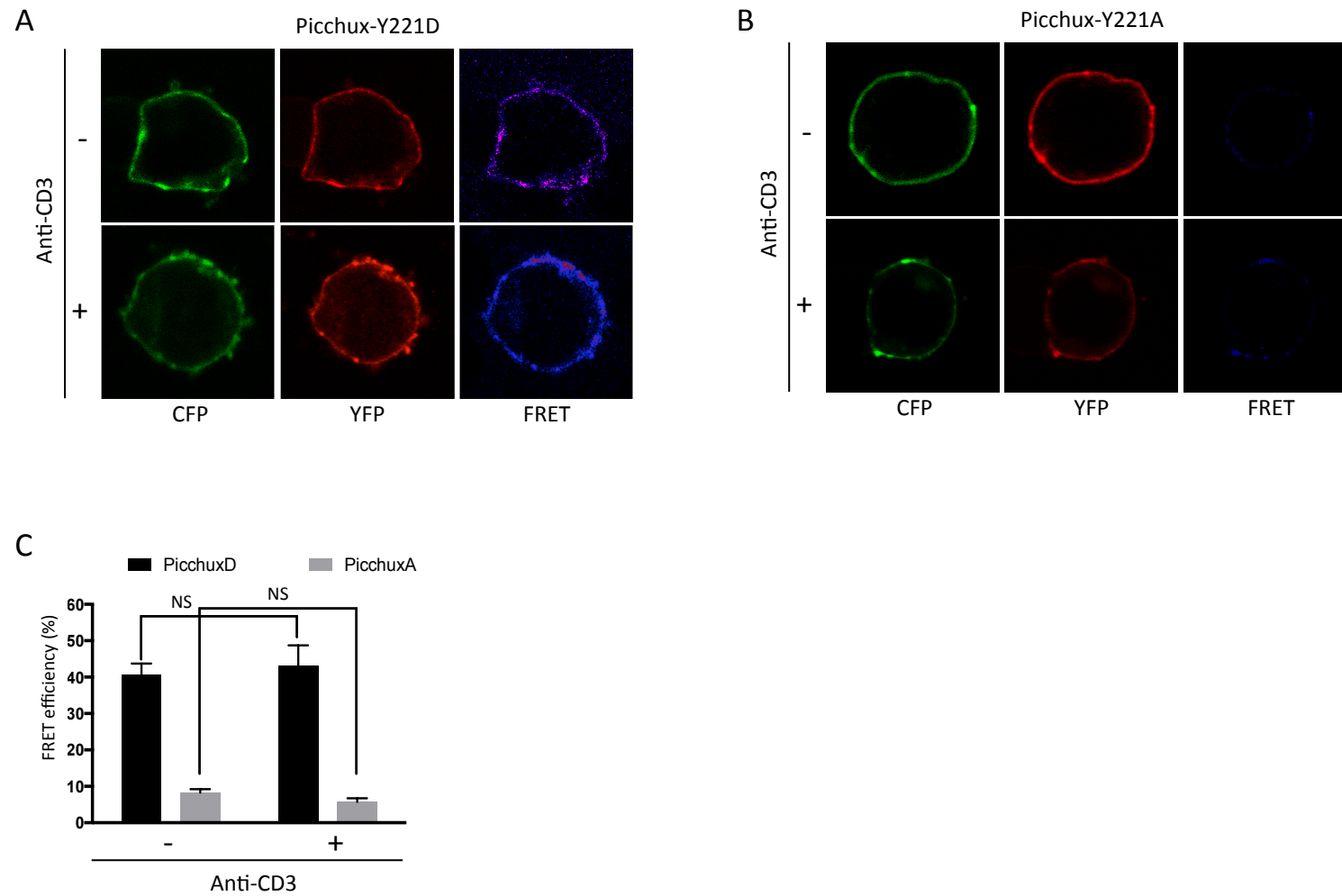
Supplementary Figure 5. *CrkII* interacts with both *C3G* and *CasL*.



Supplementary Figure 6. *Pervanadate treatment results in phosphorylation of CrkII at position 221.*



Supplementary Figure 7. *Stimulation via the T cell receptor leads to recruitment of Crkl to the membranous fraction.*



Supplementary Figure 8. *PicchuX-Y221D* construct is folded prior to stimulation.